Review

Marina Evich, Alexander M. Spring-Connell and Markus W. Germann*

Impact of modified ribose sugars on nucleic acid conformation and function

DOI 10.1515/hc-2017-0056
Received March 17, 2017; accepted April 25, 2017; previously published online June 3, 2017

Abstract: The modification of the ribofuranose in nucleic acids is a widespread method of manipulating the activity of nucleic acids. These alterations, however, impact the local conformation and chemical reactivity of the sugar. Changes in the conformation and dynamics of the sugar moiety alter the local and potentially global structure and plasticity of nucleic acids, which in turn contributes to recognition, binding of ligands and enzymatic activity of proteins. This review article introduces the conformational properties of the (deoxy)ribofuranose ring and then explores sugar modifications and how they impact local and global structure and dynamics in nucleic acids.

Keywords: deoxyribose; nucleic acids; nucleic acid modification; pseudorotation; ribose; sugar conformation.

Introduction

Nucleic acids contain the genetic information for life. While the primary information is encoded in the sequence of the nucleobases, the global and local conformation, accessibility and structural plasticity contribute to recognition by proteins and drugs. Controlling the readout of the genetic information has tremendous implications for combatting a multitude of diseases. Thus, nucleic acids based technologies for therapeutics and nanotechnologies have garnered much interest. These technologies, enabled by the ease of oligonucleotides synthesis, include plasmid-based gene therapies, antisense, short interfering RNA (siRNA), short hairpin RNA (shRNA), aptamers and other nucleic acid based therapeutics [1–6]. However, natural DNA or RNA itself is not suitable because of degradation, low binding affinities and poor cellular uptake. The introduction of chemically modified oligonucleotides overcome some of these limitations and introduces unique properties. Thus, many chemical modifications have been made to bases, the ribose sugar and the sugar-phosphodiester backbone to improve their properties for different applications.

Here we focus on the effect of ribofuranose modifications that change the local sugar conformation (Figure 1). The conformation and dynamics of the sugar moiety affect the local and potentially global structure and plasticity of nucleic acids, which contributes to recognition, binding of ligands and enzymatic activity of proteins. Through both endogenous and exogenous events, the (deoxy) ribose sugars are subjected to many modifications that alter structure and stability. Understanding the consequences of such structural perturbations are crucial in the design of DNA/RNA targeting drugs. 2′-Modifications, for example, often improve nuclease resistance, whereas the introduction of a methylene bridge in locked nucleic acids (LNA) greatly increases thermal stability.

This review article is separated into three parts, the first section introduces the conformational properties of the (deoxy)ribofuranose ring, while the remaining sections each describe modifications and effects to the cyclic sugar atoms: the 4′-O cyclic oxygen and the C1′-C4′ atoms. Base modifications and modifications that replace the furanose are covered in other reviews [7–10].

Ribose conformation: description, determination, dynamics and effect on local and global geometry

The ribofuranose sugar consists of a pentose ring (C1′, C2′, C3′, C4′, and O4′) and an exocyclic CH_2OH group (C5′) (Figure 1). The nucleobase is attached at the anomeric C1′ carbon which is canonically found in the β configuration

***Corresponding author: Markus W. Germann,** Georgia State University, Department of Chemistry, 50 Decatur St. SE, Atlanta, GA 30303, USA; Georgia State University, Department of Biology, P.O. 4010, Atlanta, GA 30303, USA; Georgia State University, Neuroscience Institute, P.O. 5030, Atlanta, GA 30303, USA, e-mail: mwg@gsu.edu
Marina Evich and Alexander M. Spring-Connell: Georgia State University, Department of Chemistry, 50 Decatur St. SE, Atlanta, GA 30303, USA

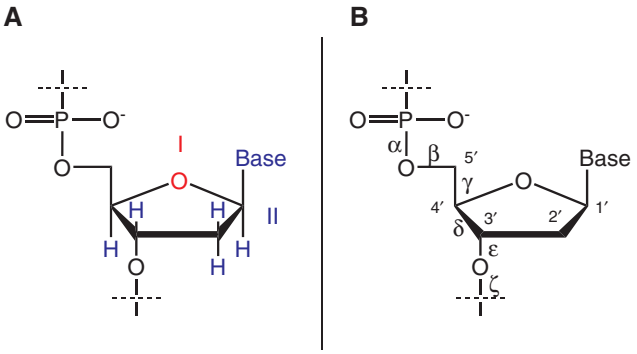

Figure 1 (A) Modifications to deoxyribonucleotide, including changes to the endocyclic oxygen (I) and the C1′-C4′ atoms (II) covered in this review. (B) Sugar carbons are labeled 1′-5′and backbone torsion angles are described as follows:

α = O3′(i−1)-P-O5′-C5′

β = P-O5′-C5′-C4′

γ = O5′-C5′-C4′-C3′

δ = C5′-C4′-C3′-O3′

ε = C4′-C3′-O3′-P (i+1)

ζ = C3′-O3′-P (i+1)-O5′(i+1)

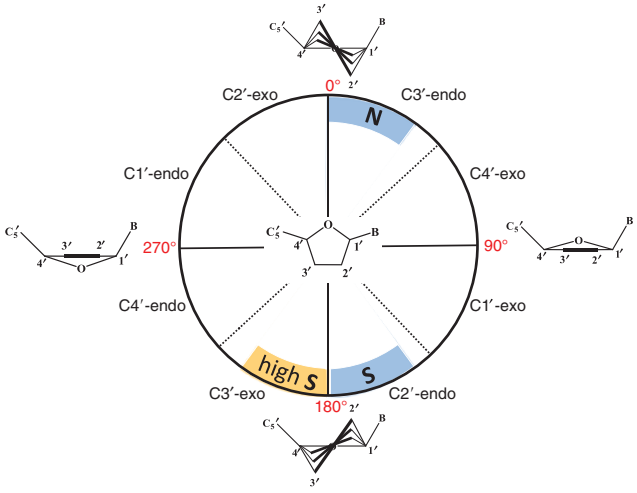

Figure 2 Pseudorotation wheel, adopted from Altona and Sundaralingam [11]. The faces of the sugar ring are defined as endo on the C5′ side and exo on the C3′ oxygen side of the sugar ring. Examples of amplitude changes are characterized on the C3′-endo and C2′-endo pucker examples. N ranges from 0 to 36 degrees and S ranges from 144 to 180 degrees [11]. Sugar torsion angles, P, and Θm are defined as:

$\nu 0$ = C4′-O4′-C1′-C2′

$\nu 1$ = O4′-C1′-C2′-C3′

$\nu 2$ = C1′-C2′-C3′-C4′

$\nu 3$ = C2′-C3′-C4′-O4′

$\nu 4$ = C3′-C4′-O4′-C1′

$$\tan P = \frac{(\nu_4 + \nu_1) - (\nu_3 + \nu_0)}{2\nu_2(\sin 36^\circ + \sin 72^\circ)} \quad \text{and} \quad \theta_M = \frac{\nu_2}{\cos P}$$

positioning the base on the endo face. The C5′ oxygen and the C3′ oxygen are linked by phosphodiester bonds orienting the plane of the sugar parallel to the nucleic acid backbone. In a double helix, the sugar substituents are therefore located either on the backbone (i.e. the 3′, 4′, and 5′/5″ substituents), in the major groove (2′), or in the minor groove (1′). The placement of the 2″ substituent is dependent on conformational changes in the sugar which differ for DNA and RNA (*vide infra*).

The ribofuranose ring is not flat but is puckered (Figure 2). The overall conformation of the pucker is defined by five endocyclic torsion angles. These angles are conveniently combined to yield the characteristic pseudorotation angle (P) where all sugar conformational states can be identified by a unique P-value. The sugar ring is further defined by the amplitude of the pucker (θ_M) [11] (Figure 2). In nucleic acid duplexes, steric forces and electronegative characteristics of the sugar substituents result in two predominate conformations: C2′-endo (a P of 144 to 180° also known as south or S) and C3′-endo (a P of 0 to 36° also known as north or N). The sugar moieties for RNA and DNA differ by only one atom: the 2″ functional group: a hydroxyl (-OH) for RNA and a hydrogen atom (-H) for DNA. This subtle difference has a profound impact on the sugar conformation. Steric hindrance and electrostatic interactions between the 3′ oxygen and the 2″ hydroxyl group of the RNA drive the conformation to an N pucker whereas in DNA, the S conformation is favored with the 2″ hydrogen. In RNA, the N conformation places the 2″ hydroxyl in the minor groove; for DNA, the placement of the 2″ -H is dependent on variations in P and θ_M.

The sugar pucker is not static but exists in a dynamic equilibrium between the S and N states, often characterized as a fraction of the S conformation (f_s). The populations, energetics and timescale of interconversion between the S and N states have profound impacts on the local and global duplex conformation and protein recognition. Several NMR techniques exist that can give insight into the f_S of the sugar pucker equilibrium as well as the pseudorotation (P) and amplitude (θ_M) of the dominate form. The most widespread method is through the analysis of 3-bond scalar couplings (^3J) of the sugar protons through NMR ^{1}H-^{1}H COSY experiments. These values are highly dependent on torsion angles via the Karplus relationships and correlate well to the overall pseudorotation angle [12–21]. Other NMR techniques used to evaluate the sugar pucker include ^{1}H-^{1}H NOESY crosspeak analysis, ^{13}C chemical shifts evaluation of C3′, and heteronuclear ^{13}C-^{1}H coupling values [22–26].

Table 1 Difference in Gibbs Free energy (ΔG) between the N and S conformations as a function of temperature and population ratios.

Temp. (°C)	Ratio S/N		
	60/40	80/20	95/5
5	0.22	0.77	1.63
25	0.24	0.82	1.74
37	0.25	0.85	1.81
65	0.27	0.93	1.98

The left column represents the temperature in °C; the right three columns are the calculated ΔG (kcal/mol) between the N and S conformations for the population distributions indicated on the first row of the table. ($\Delta G = -RT \times \ln K$, where K is defined as the ratio of S to N).

The energetic barrier between the S and N states is determined by the ratio of the populations and is relatively temperature independent (Table 1). The f_S is highly dependent on the nucleobase sequence and sugar ring substituents [27, 28]. The rate of sugar conformation interconversion occurs on the ps to ns time frame [29, 30]. ^{13}C NMR combined with molecular dynamics simulations have been used to probe the timescale of A-track DNA sugar puckering dynamics via the evaluation of longitudinal and transverse relaxation rates (T_1 and T_2, respectively) of C1′ [30]. Aside from this method, the primary methods for exploring the timescale are via computational approaches. Our lab has used NMR and molecular dynamics simulations to determine the sugar conformation and assess the dynamics of S/N interconversion. Pseudorotation analysis of a single riboguanosine in a DNA duplex, probed by free molecular dynamics simulations revealed that the presence of a single hydroxyl group rigidifies the ribose sugar, inducing a conformation switch from S to N and changes the sugar dynamics from a ps to ns timescale, Figure 4 (Germann laboratory, unpublished data).

Sugar puckering also has a profound impact on the global duplex conformation due to the C3′-C4′-C5′ backbone connectivity. The S sugar pucker places the C5′ and C3′ atoms far apart from one another allowing for well-spaced phosphorus atoms and the canonical B-type global helical conformation found in DNA. In contrast, the N sugar pucker of RNA brings the C3′ and C5′ atoms closer together yielding a closer spacing of the phosphorus atoms and results in the more compact A-type global helical conformation. (P_n to P_{n+1} distances are ~5.8 and ~7 Å, respectively for canonical A-type and B-type double helical nucleic acids) [31]. The sugar conformation and interconversion impacts several helical parameters as well as the conformational sampling of backbone geometries [27, 32]. Among others, the ε and ζ torsion angles (ε = C4′-C3′-O3′-P and ζ = C3′-O3′-P-O5′), which define the B_I and B_{II} backbone conformational states, have been found to be somewhat linked to sugar pucker changes. B_I and B_{II} characterize the overall backbone geometry of the double helix where B_I is defined as ε in a trans configuration and ζ in a gauche – configuration and B_{II} with ε in gauche – and ζ in trans configurations. More importantly, however, the B_I and B_{II} torsion angle populations and dynamic interconversion are major determinants of the intrinsic flexibility and arrangement of the backbone and are thus crucial factors in protein recognition and binding [33, 34].

Chemical modifications of the ribofuranose are expected to change the local sugar conformation and dynamics, which impacts recognition and stability and can be used to modulate specific interactions and properties of oligonucleotides. Common modifications which affect the sugar ring are discussed in the following sections.

Furanose ring: 4′-O to sulfur or selenium

The oxygen of the furanose ring can be replaced with sulfur and selenium to yield 4′-thio and 4′-selenonucleotides. The sulfur analog is significantly more lipophilic than the natural counterpart [35, 36]. These modifications impart unique properties making them attractive candidates for PCR, RNA aptamer post-modification and siRNA, antisense technology and assisting in phasing X-ray crystallographic data [35, 37–41].

Free nucleosides with either of these modifications exhibit a southern sugar conformation, however, duplexes containing singly or uniformly modified residues exhibit northern characteristics. Depending on the extent of the modification, (i.e. single or isolated, stretches of modifications, or uniformly modified duplexes or hybrids with 4′-thionucleotides (4′-thioRNA) or 2′-deoxy-4′-thionucleotides (4′-thioDNA) in duplexes) 4′-thionucleotides impart stabilizing or destabilizing effects and varying nuclease resistance. For example, a Dickerson-Dodecamer duplex containing two consecutive 4′-thioDNA thymine residues (per strand) is globally still in a B-form but exhibits local conformational changes primarily 5′ of the modifications on each strand. This includes a shift in pseudorotation angle, P, to ~200° (towards C3′-exo) as compared to the analogous thymine control residues (116°, C1′-exo), coupled with minor changes in

backbone torsion angles and changes in helical rise, twist and groove dimensions [42].

Further studies with isolated 4′-thioDNA nucleotides in DNA duplexes (one to two per strand in self-complementary duplexes), similarly found that the global structure remained B-form from CD analysis. However, depending on sequence environment, isolated 4′-thioDNA residues either decrease or increase the thermal stability ($\Delta T_m = -5$ to +3°C), with varied endonuclease resistance [43]. Uniformly modified 4′-thioDNA oligonucleotides result in A-form DNA, with most sugars in C3′-endo conformations. The full conformation switch (B→A-form), observed by NMR is believed to be due to difference in hydrophobicity of sulfur, which compared to oxygen, disrupts the hydration spine, providing a dehydrating environment. This conformational switch was further supported by preferential binding of RNA groove binding drugs rather than DNA groove binders, nuclease resistance and preferential hybridization to RNA strands [44, 45]. The 4′-thioRNA modified hybrids and duplexes retain global A-form characteristics, due to the 2′ hydroxyl, while contributing thermal stability of up to 2.5°C/base pair and contribute nuclease resistance to RNA duplexes [39]. To our knowledge, no structural data exists to confirm the sugar conformation of a partially or fully modified 4′-selenonucleotide (4′-SeRNA) or 2′-deoxy-4′-selenonucleotide (4′-SeDNA). However, evidence exists that isolated 4′-SeRNA modifications in RNA and DNA behave like ribonucleotides, based on CD and thermal melting studies [35].

Furanose ring C1′ modifications: abasic, α anomeric residues

An extreme C1′ modification is the removal of the nucleobase (Figure 3). This extensive change affects the conformational properties of the remaining sugar and impacts surrounding residues. Abasic sites are a common form of DNA damage resulting from spontaneous or enzyme induced cleavage of the glycosidic bond [46–48]. This lesion is toxic to cells and is further processed and repaired by the base excision repair pathway. Abasic sites are chemically intrinsically labile; they mainly exist as a mixture of α/β hemiacetals with a small amount (<1%) of ring opened aldehyde hydrate [49, 50]. The aldehyde form may lead to a DNA strand break; earlier work therefore often used the more stable tetrahydrofuran (THF) analog (Figure 3) to study the effect of abasic sites [51–54]. In MD simulations of DNA duplexes with a THF analog, the abasic sugar analog exhibited a broad range of conformations centered around the northern pucker, suggesting significant conformational flexibility, due to the absence of base pairing and stacking interactions [53]. A more recent NMR study on two DNA duplexes containing a single THF analog on each strand, offset by one nucleotide, found that of the four THF abasic analog sites in these two duplexes, three were predominantly in a southern conformation and one exhibited a northern pucker, indicating position/sequence dependence [54]. Chen et al. [55] have used uracil glycosylase to create an abasic site *in situ* in a DNA duplex . The resulting hemiacetal rings had a 60:40 ratio of α to β anomers with N- and S-type conformations, respectively. THF is a convenient and stable abasic analog, however, in contrast to an actual abasic site, it is missing a hydroxyl group, which exists in an α/β orientation.

Inversion of the stereochemistry at the C1′ position results in α anomeric nucleosides (Figure 3). The sugar conformation of the nucleosides (αA, αC, αG & αT) are all reported to be in the southern range (P, 155°–174°) with a reduced puckering amplitude [56]. α anomeric DNA lesions may arise in DNA via the abstraction of the anomeric hydrogen by a hydroxyl radical under anoxic condition [57]. In 1973, Sequin predicted that an α anomeric DNA oligomer forms a duplex with a complementary

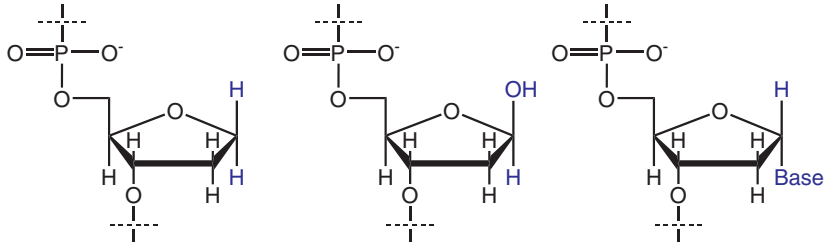

Figure 3 Extreme C1′ modifications include: a tetrahydrofuran (THF), an apurinic/apyrimidinic (AP) or oxidized abasic site with a missing base at the β position of the C1′ carbon, and an α-anomer, with inverted stereochemistry of the base at C1′.

β- or α-strand by Watson-Crick base pairing and the two strands should exhibit parallel and antiparallel polarity, respectively [58]. This was subsequently experimentally demonstrated by Imbachs group for α/β DNA, α/α DNA double helices [59, 60]. In the antiparallel α/α and parallel α/β DNA duplexes, the sugar puckering of the α anomeric sugars are reported as C3′-exo (S-type) with a reduced puckering amplitude [61, 62]. Embedding a single α anomeric nucleotide in an oligonucleotide duplexes with a DNA complement revealed a reversed Watson-Crick base pair orientation and a high S sugar conformation [63, 64]. Our laboratory has also investigated single α anomeric residues that are embedded via 3′3′ and 5′5′ linkages in otherwise natural oligonucleotides. In these constructs, the α anomeric residue (αA, αC, αG, αT) forms a Watson-Crick base pair with a complementary DNA or RNA strand in a local parallel stranded orientation [65, 66]. The sugar conformation of the α anomeric sugars are in the high S range (P, 200–225, C3′-exo) with reduced puckering amplitude similar to the free nucleosides [67]. Dynamics simulations further supported the high preference for a C3′-exo conformational preference and indicated that compared to surrounding β anomeric sugars α anomeric sugars are rigid and less dynamic [68].

Furanose ring C2′ modifications: H to -OH, -OCH_3, -F, -$SeCH_3$, LNA

A key distinction between DNA and RNA is the presence of a single hydroxyl group in place of a hydrogen atom at the C2′ position in the sugar ring. A fully modified duplex, i.e. RNA, has sugars adopting rigid C3′-endo sugar puckers, resulting in an A-form helix. However, depending on the number of modifications and the flanking nucleotides, different conformational shifts have been reported. Typically, DNA/RNA hybrids display features of both A- and B-forms, but are overall more like A-form duplexes, with sugars of the RNA strand primarily in C3′-endo puckers, while the DNA strand of the hybrid exhibits more plasticity, with flexible sugars in C2′-endo conformations. Ribonucleotides present in DNA represent the most common non-standard nucleotide and outnumber any other form

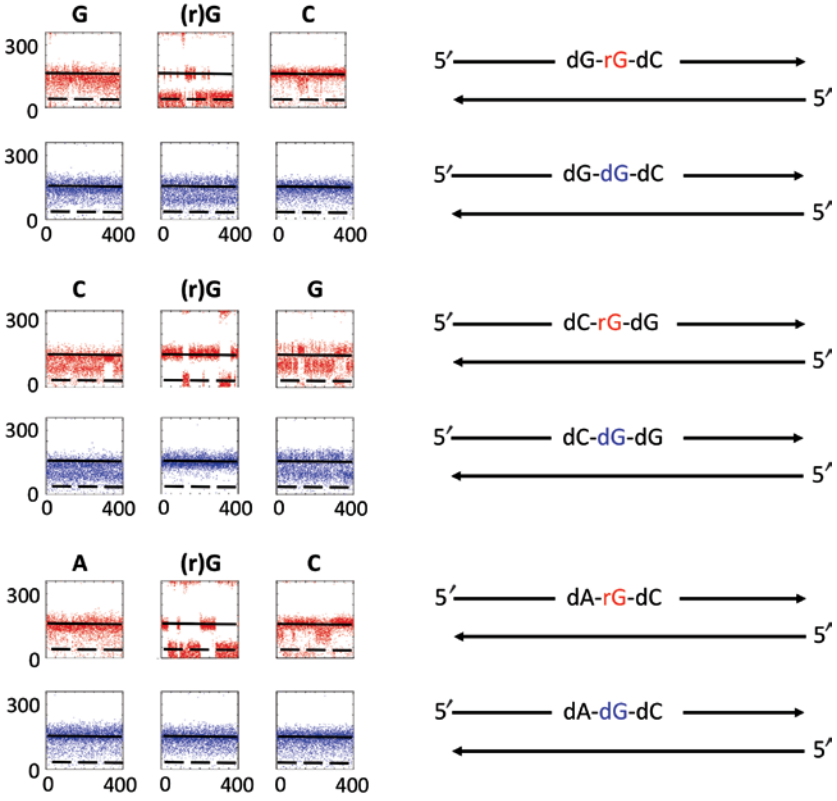

Figure 4 Molecular dynamics (MD) traces of pseudorotational phase angle (P) values, in degrees, as a function of simulation time, in ns for three single riboguanosine-containing DNA duplexes (red) and corresponding all DNA controls (blue), focusing on the core sugars. Unrestrained MD simulations were run in Amber 14 with the parmBSC0 forcefield with ε/ζ reparameterizations [72, 73]. An average south conformation is denoted by a solid line, and an average north is represented by a dashed line.

of DNA damage [69]. Single or isolated ribonucleotides introduced into genomic DNA either through endogenous cellular processes or through environmental factors leave the DNA in an overall B-form structure, in contrast to stretches of ribonucleotides like in DNA/RNA hybrids or chimeric oligonucleotides [70]. However, the presence of a single ribonucleotide in a DNA duplex affects the local sugar conformations asymmetrically and in a sequence dependent manner, as determined by NMR [71]. The incorporated ribonucleotide exists in 40%–60% f_S conformations, which is modulated by the neighboring residues, and also has subtle effects on backbone torsion angles. Computational methods confirm the sequence dependent effect on the sugar conformational repertoire of a single riboguanosine observed by NMR and further reveal a change in the dynamics from a ps to ns timescale (Figure 4).

Other modifications at the C2′ position, such as 2′-*O*-alkyl, enhance nuclease resistance of RNA and for example, increase the siRNA half-life and therapeutic potential in cells and animals while retaining comparable activities relative to unmodified siRNAs [74, 75]. 2′-Position modified analogs are also attractive antisense therapy lead molecules in part due to the removal of the 2′-hydroxyl group which renders the RNA vulnerable to strand cleavage by bases and enzymes [76]. The introduction of 2′-methoxy modifications in DNA shift sugar conformations to C3′-endo. Additional stabilizing forces for methoxy RNA/RNA duplexes may arise from base stacking and hydrophobic interactions of methoxy groups in the minor groove [77].

C2′ fluorine substituents have the added benefit of being readily monitored by NMR. Depending on the attachment at C2′, fluorine switches the sugar pucker due to its electronegativity; the polarity of this substitution determines the sugar conformation rather than its size, as it is similar to hydrogen [78]. Nucleosides with single fluorine substitutions at the 2′ carbon position in the *ribo* configuration favor C3′-endo conformations and the *ara* residues prefer C2′-endo (Figure 5) [79]. In both cases, the absence of the 2′-hydroxyl group results in increased chemical stability and nuclease resistance. Oligonucleotides with fluorines in either the *ribo* (with northern conformations) or *ara* position (which exhibits more eastern conformation) have higher affinity for RNA compared to unmodified DNA or RNA oligonucleotides [80, 81]. Duplexes of uniformly modified 2′-fluorinated (*ribo*) oligonucleotides hybridized to RNA strands are not RNase H substrates while the *ara* analogs retain RNase H activity [81, 82]. These traits, together with low nonspecific binding to cellular proteins, render them effective in antisense, gene silencing and gene expression applications

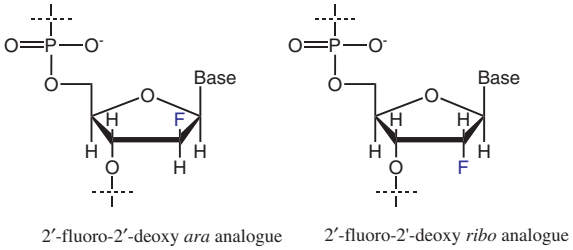

Figure 5 Single fluorine modifications in the *ara* or *ribo* positions at the C2′ carbon. A fluorine modification at the *ara* position has a propensity for the C2′-endo sugar conformation, while a fluorine at the *ribo* position, favors a C3′-endo conformation.

[83, 84]. Chimeric siRNA duplexes containing mixtures of both *ribo* and *ara* fluorinated variants have been shown to effectively silence genes [81]. As anticipated from the bias in sugar puckering, partially modified B-form DNA duplexes with 2′-fluoro *ribo* substituents have destabilizing effects while the *ara* modifications have stabilizing effects of +2°C/modification [85, 86].

2′-Se-methyl modifications are chemically stable and assist in the phase determination in X-ray crystallography. In addition, for RNA- and A-form DNA duplexes this modification also may facilitate crystallization. In these crystalized duplexes, the modified sugar maintains a C3′-endo sugar conformation [87–89]. However, others have also noted failed crystallization attempts with Se-modified DNA [76]. In contrast to -OH or -F modifications, the S conformation is preferred for -Se-CH_3 by 84% in a nucleoside, suggesting that a B helical structure should be compatible and even stabilized by this modification [90]. Nevertheless, if placed in a DNA duplex, this modification profoundly destabilizes B form DNA in solution and results in the formation of multiple species (duplex and hairpin structures). Molecular modeling, augmented by NMR, fluorescence and melting studies, indicate that steric clashes of the 2′-Se-CH_3 moiety with the phosphodiester backbone and the nucleobase effectively destabilizes a B helix [90]. In an A form duplex, that group is comfortably nestled in the minor groove and may aid dehydration to promote A helix formation and crystallization (Figure 6).

The sugar moiety can also be ‘locked’ into a specific conformation via a covalent bridge. Commonly, locked nucleic acids (LNA) typically refer to the RNA mimics, where the ribose 2′- oxygen atom is connected to the 4′-carbon by a methylene bridge, but variants including 2′- sulfur or amine groups (thio-LNA, amino-LNA) have also been reported [91, 92]. Traditional locked nucleic acids are either the β-D-*ribo* LNA (commonly referred to as LNA) or the less common α-L-*ribo* LNA conformer

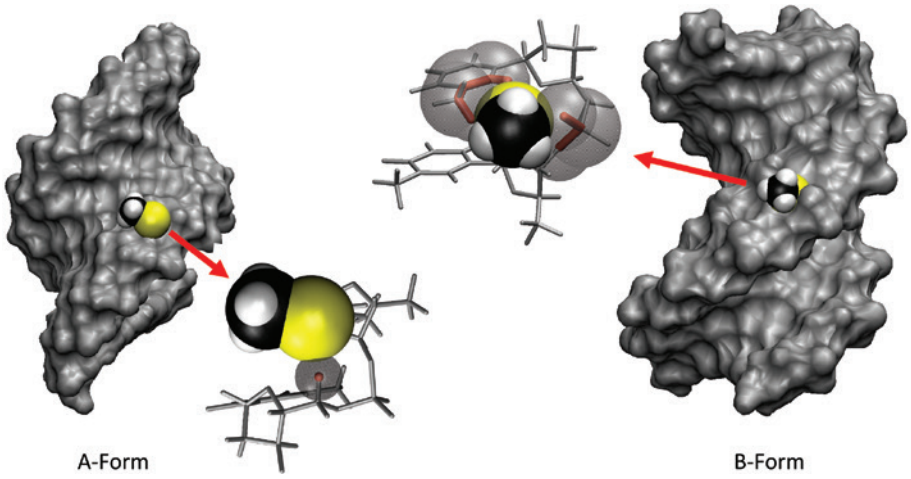

Figure 6 Positioning of 2′-Se-methyl group in A and B form helices. In an A form duplex (left) the moiety is nestled in the minor groove, there is minimal steric interference (H of a 5′ CH_2 group). In contrast, in a B type helix where the group points into the major groove, there are clashes with both base (methyl and H6) and backbone (O, P) atoms. Atoms with clashes are labeled red and VdW representation of selenium are shown in yellow, the methyl carbon is black and the hydrogens are in white.

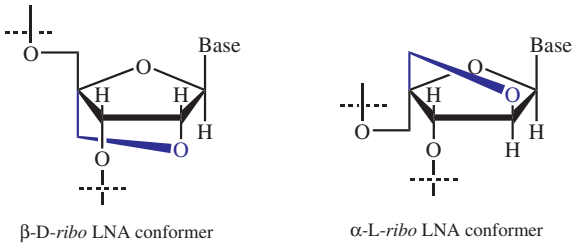

Figure 7 Locked nucleic acid conformers containing a methylene bridge linking ribose 2′-O and 4′-C. The more common LNA typically refers to the RNA mimic, β-D-*ribo* LNA. Alternatively, α-L-*ribo* LNA locks the sugar in a C2′-endo conformation.

(Figure 7). The α-L-*ribo* LNA results in a C2′-endo conformation, stabilizing B-form duplexes, making this modification useful in triplex-forming oligonucleotides and other studies where B-form DNA is required [93, 94]. Alternatively, the β-D-*ribo* LNA (LNA) isomer imparts rigidity and stability to the oligonucleotide; the ribose sugar is fixed in a C3′-endo conformation and thermal stability increases up to several degrees per LNA residue [95]. In addition, LNA also provides good mismatch discrimination, low toxicity and nuclease stability. Studies have investigated fully modified LNA and LNA 'mixmers' with LNA and DNA residues in different combinations [96]. In diagnostics and therapeutics LNA uses include detection of single nucleotide polymorphisms (SNPs) with PCR and antisense approaches [96–98]. A limitation of the use of LNA is the lack of certain commercially available phosphoramidites: there currently are no uracil or cytosine phosphoramidites [96]. Thymine and 5-methylcytosine are available.

Summary and outlook

We focused on modifications to the furanose sugar moiety, however alterations to the bases and backbone can modulate the sugar conformation and impact lipophilicity, nuclease resistance and DNA/RNA binding affinity. For example, unusual linkages such as 3′,3′ and 5′,5′ linkages investigated in our laboratories affect the distribution and dynamics of sugar puckering [56, 68, 99]. Modifications on the non-linking phosphate oxygen atoms, such as boranophosphonate, phosphorothioate, phosphorodithioates and methylphosphonates have been used as potential gene regulators for antisense technologies. These modifications can induce local sugar conformation switches, depending on the stereochemistry of the modifications [100–107]. The sugar conformation depends on substituents that alter hydrophobicity affecting hydration or by introducing electronegative and/or bulky modifications at the 2′-position. Furthermore, the sequence environment (Figure 4), as well as damaged bases affect the sugar pucker and dynamics [108]. 8-OxoG, for example, one of the most detrimental DNA lesions, alters the local structural conformation of the sugar and backbone, promoting B_I to B_{II} changes and affects protein recognition and binding [108]. Even minor base damage can result in subtle changes in the sugar conformation ratio and dynamics, contributing to the recognition by the repair machinery. Uracil and thymine differ by only one functional group, yet this small difference yields slightly different nucleotide dynamics and conformational equilibria [109].

Whether through intentional and designed chemical alterations or through processes that damage DNA, modifications on the DNA sugar can result in subtle to dramatic effects on the structure and properties of the molecule. A large body of experimental data augmented with molecular simulations has provided a detailed understanding of the consequences of sugar modifications both in nucleoside and in double helical structures. The fraction and rate of S/N interconversion has remarkable impact on the local conformation and stability of the DNA structure, protein recognition and enzyme function. This insight can be exploited to readily select desired sugar conformations and dynamics to modulate substrate affinity and stability for different biotechnological applications. The ease of chemical synthesis of oligonucleotides, and the commercial availability of many modified phosphoramidites, has resulted in an astounding number of publications in recent decades on DNA-based therapeutics.

Acknowledgements: M.E. is supported by the Brains and Behavior program from GSU. Part of this work was supported by the Georgia Cancer Coalition and NIH (GM55404-01A1).

References

[1] Vorburger, S. A.; Hunt, K. K. Adenoviral gene therapy. *Oncologist* **2002**, *7*, 46–59.
[2] Evers, M. M.; Toonen, L. J. A.; van Roon-Mom, W. M. C. Antisense oligonucleotides in therapy for neurodegenerative disorders. *Adv. Drug Delivery Rev.* **2015**, *87*, 90–103.
[3] Kanasty, R.; Dorkin, J. R.; Vegas, A.; Anderson, D. Delivery materials for siRNA therapeutics. *Nat. Mater.* **2013**, *12*, 967–977.
[4] Moore, C. B.; Guthrie, E. H.; Huang, M. T.-H.; Taxman, D. J. Short hairpin RNA (shRNA): design, delivery, and assessment of gene knockdown. *Methods Mol. Biol.* **2010**, *629*, 141–158.
[5] Keefe, A. D.; Pai, S.; Ellington, A. Aptamers as therapeutics. *Nat. Rev. Drug Discov.* **2010**, *9*, 537–550.
[6] Alvarez-Salas, L. M. Nucleic acids as therapeutic agents. *Curr. Top. Med. Chem.* **2008**, *8*, 1379–1404.
[7] Plongthongkum, N.; Diep, D. H.; Zhang, K. Advances in the profiling of DNA modifications: cytosine methylation and beyond. *Nat. Rev. Genet.* **2014**, *15*, 647–661.
[8] Rozners, E. Recent advances in chemical modification of peptide nucleic acids. *J. Nucleic Acids* **2012**, *2012*, 518162.
[9] Watts, J. K.; Deleavey, G. F.; Damha, M. J. Chemically modified siRNA: tools and applications. *Drug Discov. Today* **2008**, *13*, 842–855.
[10] Corey, D. R. Chemical modification: the key to clinical application of RNA interference? *J. Clin. Invest.* **2007**, *117*, 3615–3622.
[11] Altona, C.; Sundaralingam, M. Conformational analysis of the sugar ring in nucleosides and nucleotides. A new description using the concept of pseudorotation. *J. Am. Chem. Soc.* **1972**, *94*, 8205–8212.
[12] Karplus, M.; Grant, D. M. A criterion for orbital hybridization and charge distribution in chemical bonds. *Proc. Natl. Acad. Sci. USA.* **1959**, *45*, 1269–1273.
[13] Karplus, M. Vicinal proton coupling in Nuclear Magnetic Resonance. *J. Am. Chem. Soc.* **1963**, *85*, 2870–2871.
[14] Wüthrich, K. NMR of Proteins and Nucleic Acids; John Wiley & Sons, Inc: Canada, 1986; p 292.
[15] De Leeuw, F. A.; Altona, C. Component vicinal coupling constants for calculating side-chain conformations in amino acids. *Int. J. Pept. Protein Res.* **1982**, *20*, 120–125.
[16] Bax, A.; Lerner, L. Measurement of 1H-1H coupling constants in DNA fragments by 2D NMR. *J. Magn. Reson.* **1988**, *79*, 429–438.
[17] van Wijk, J.; Huckriede, B. D.; Ippel, J. H.; Altona, C. Furanose sugar conformations in DNA from NMR coupling constants. *Methods Enzymol.* **1992**, *211*, 286–306.
[18] Rinkel, L. J.; Altona, C. Conformational analysis of the deoxyribofuranose ring in DNA by means of sums of proton-proton coupling constants: a graphical method. *J. Biomol. Struct. Dyn.* **1987**, *4*, 621–649.
[19] Cordier, C.; Marcourt, L.; Petitjean, M.; Dodin, G. Conformational variation of the central CG site in d(ATGACGTCAT)2 and d(GAAAACGTTTTC)2. An NMR, molecular modelling and 3D-homology investigation. *Eur. J. Biochem.* **1999**, *261*, 722–733.
[20] de Leeuw, F. A., Altona, C. Quantum Chemistry Program Exchange, no. 463: PSEUROT 3B; Indiana University, Bloomington, IN, 1983.
[21] Widmer, H.; Wüthrich, K. Simulated two-dimensional nmr cross-peak fine structures for 1H spin systems in polypeptides and polydeoxynucleotides. *J. Magn. Reson.* **1987**, *74*, 316–336.
[22] Chary, K. V.; Modi, S. Analysis of intrasugar interproton NOESY cross-peaks as an aid to determine sugar geometries in DNA fragments. *FEBS Lett.* **1988**, *233*, 319–325.
[23] Denisov, A. Y.; Noronha, A. M.; Wilds, C. J.; Trempe, J. F.; Pon, R. T.; Gehring, K.; Damha, M. J. Solution structure of an arabinonucleic acid (ANA)/RNA duplex in a chimeric hairpin: comparison with 2′-fluoro-ANA/RNA and DNA/RNA hybrids. *Nucleic Acids Res.* **2001**, *29*, 4284–4293.
[24] Suardiaz, R.; Sahakyan, A. B.; Vendruscolo, M. A geometrical parametrization of C1′-C5′ RNA ribose chemical shifts calculated by density functional theory. *J. Chem. Phys.* **2013**, *139*, 034101.
[25] Vokacova, Z.; Bickelhaupt, F. M.; Sponer, J.; Sychrovsky, V. Structural interpretation of J coupling constants in guanosine and deoxyguanosine: modeling the effects of sugar pucker, backbone conformation, and base pairing. *J. Phys. Chem. A* **2009**, *113*, 8379–8386.
[26] Dejaegere, A. P.; Case, D. A. Density functional atudy of ribose and deoxyribose chemical shifts. *J. Phys. Chem. A* **1998**, *102*, 5280–5289.
[27] Packer, M. J.; Dauncey, M. P.; Hunter, C. A. Sequence-dependent DNA structure: tetranucleotide conformational maps. *J. Mol. Biol.* **2000**, *295*, 85–103.
[28] Olson, W. K.; Gorin, A. A.; Lu, X. J.; Hock, L. M.; Zhurkin, V. B. DNA sequence-dependent deformability deduced from protein-DNA crystal complexes. *Proc. Natl. Acad. Sci. USA.* **1998**, *95*, 11163–11168.
[29] Borer, P. N.; LaPlante, S. R.; Kumar, A.; Zanatta, N.; Martin, A.; Hakkinen, A.; Levy, G. C. 13C-NMR relaxation in three DNA

oligonucleotide duplexes: model-free analysis of internal and overall motion. *Biochemistry* **1994**, *33*, 2441–2450.
[30] Nikolova, E. N.; Bascom, G. D.; Andricioaei, I.; Al-Hashimi, H. M. Probing sequence-specific DNA flexibility in a-tracts and pyrimidine-purine steps by nuclear magnetic resonance C relaxation and molecular dynamics simulations. *Biochemistry* **2012**, *51*, 8654–8664.
[31] Rich, A. The double helix: a tale of two puckers. *Nat. Struct. Biol.* **2003**, *10*, 247–249.
[32] Ben Imeddourene, A.; Elbahnsi, A.; Gueroult, M.; Oguey, C.; Foloppe, N.; Hartmann, B. Simulations meet experiment to reveal new insights into DNA intrinsic mechanics. *PLoS Comput. Biol.* **2015**, *11*, e1004631.
[33] Robertson, J. C.; Cheatham, T. E. DNA backbone BI/BII distribution and dynamics in E2 protein-bound environment determined by molecular dynamics simulations. *J. Phys. Chem. B* **2015**, *119*, 14111–14119.
[34] Heddi, B.; Foloppe, N.; Bouchemal, N.; Hantz, E.; Hartmann, B. Quantification of DNA BI/BII backbone states in solution. Implications for DNA overall structure and recognition. *J. Am. Chem. Soc.* **2006**, *128*, 9170–9177.
[35] Watts, J. K.; Johnston, B. D.; Jayakanthan, K.; Wahba, A. S.; Pinto, B. M.; Damha, M. J. Synthesis and biophysical characterization of oligonucleotides containing a 4′-Selenonucleotide. *J. Am. Chem. Soc.* **2008**, *130*, 8578–8579.
[36] Koole, L. H.; Plavec, J.; Liu, H.; Vincent, B. R.; Dyson, M. R.; Coe, P. L.; Walker, R. T.; Hardy, G. W.; Rahim, S. G.; Chattopadhyaya, J. Conformation of two 4′-thio-2′-deoxynucleoside analogs studied by 5000-MHz proton NMR spectroscopy and x-ray crystallography. *J. Am. Chem. Soc.* **1992**, *114*, 9936–9943.
[37] Dande, P.; Prakash, T. P.; Sioufi, N.; Gaus, H.; Jarres, R.; Berdeja, A.; Swayze, E. E.; Griffey, R. H.; Bhat, B. Improving RNA interference in mammalian cells by 4′-thio-modified small interfering RNA (siRNA): effect on siRNA activity and nuclease stability when used in combination with 2′-O-alkyl modifications. *Eur. J. Med. Chem.* **2006**, *49*, 1624–1634.
[38] Hoshika, S.; Minakawa, N.; Shionoya, A.; Imada, K.; Ogawa, N.; Matsuda, A. Study of modification pattern-RNAi activity relationships by using siRNAs modified with 4′-thioribonucleosides. *Chembiochem* **2007**, *8*, 2133–2138.
[39] Hoshika, S.; Minakawa, N.; Matsuda, A. Synthesis and physical and physiological properties of 4′-thioRNA: application to post-modification of RNA aptamer toward NF-kappaB. *Nucleic Acids Res.* **2004**, *32*, 3815–3825.
[40] Kojima, T.; Furukawa, K.; Maruyama, H.; Inoue, N.; Tarashima, N.; Matsuda, A.; Minakawa, N. PCR amplification of 4′-thioDNA using 2′-deoxy-4′-thionucleoside 5′-triphosphates. *ACS Synth. Biol.* **2013**, *2*, 529–536.
[41] Tarashima, N.; Sumitomo, T.; Ando, H.; Furukawa, K.; Ishida, T.; Minakawa, N. Synthesis of DNA fragments containing 2[prime or minute]-deoxy-4[prime or minute]-selenonucleoside units using DNA polymerases: comparison of dNTPs with O, S and Se at the 4[prime or minute]-position in replication. *Org. Biomol. Chem.* **2015**, *13*, 6949–6952.
[42] Boggon, T. J.; Hancox, E. L.; McAuley-Hecht, K. E.; Connolly, B. A.; Hunter, W. N.; Brown, T.; Walker, R. T.; Leonard, G. A. The crystal structure analysis of d(CGCGAASSCGCG)2, a synthetic DNA dodecamer duplex containing four 4′-thio-2′-deoxythymidine nucleotides. *Nucleic Acids Res.* **1996**, *24*, 951–961.
[43] Hancox, E. L.; Connolly, B. A.; Walker, R. T. Synthesis and properties of oligodeoxynucleotides containing the analogue 2′-deoxy-4′-thiothemidine. *Nucleic Acids Res.* **1993**, *21*, 3485–3491.
[44] Matsugami, A.; Ohyama, T.; Inada, M.; Inoue, N.; Minakawa, N.; Matsuda, A.; Katahira, M. Unexpected A-form formation of 4′-thioDNA in solution, revealed by NMR, and the implications as to the mechanism of nuclease resistance. *Nucleic Acids Res.* **2008**, *36*, 1805–1812.
[45] Inoue, N.; Minakawa, N.; Matsuda, A. Synthesis and properties of 4′-ThioDNA: unexpected RNA-like behavior of 4′-ThioDNA. *Nucleic Acids Res.* **2006**, *34*, 3476–3483.
[46] Lindahl, T.; Nyberg, B. Rate of depurination of native deoxyribonucleic acid. *Biochemistry* **1972**, *11*, 3610–3618.
[47] Lindahl, T. Instability and decay of the primary structure of DNA. *Nature* **1993**, *362*, 709–715.
[48] Wallace, S. S. AP endonucleases and DNA glycosylases that recognize oxidative DNA damage. *Environ. Mol. Mutagen.* **1988**, *12*, 431–477.
[49] Manoharan, M.; Ransom, S. C.; Mazumder, A.; Gerlt, J. A.; Wilde, J. A.; Withka, J. A.; Bolton, P. H. The characterization of abasic sites in DNA heteroduplexes by site specific labeling with carbon-13. *J. Am. Chem. Soc.* **1988**, *110*, 1620–1622.
[50] Wilde, J. A.; Bolton, P. H.; Mazumder, A.; Manoharan, M.; Gerlt, J. A. Characterization of the equilibrating forms of the aldehydic abasic site in duplex DNA by oxygen-17 NMR. *J. Am. Chem. Soc.* **1989**, *111*, 1894–1896.
[51] Bailly, V.; Verly, W. G. Possible roles of beta-elimination and delta-elimination reactions in the repair of DNA containing AP (apurinic/apyrimidinic) sites in mammalian cells. *Biochem. J.* **1988**, *253*, 553–559.
[52] Ayadi, L.; Coulombeau, C.; Lavery, R. Abasic sites in duplex DNA: molecular modeling of sequence-dependent effects on conformation. *Biophys. J.* **1999**, *77*, 3218–3226.
[53] Barsky, D.; Foloppe, N.; Ahmadia, S.; Wilson, D. M.; MacKerell, A. D. New insights into the structure of abasic DNA from molecular dynamics simulations. *Nucleic Acids Res.* **2000**, *28*, 2613–2626.
[54] Hazel, R. D.; Tian, K.; de los Santos, C. NMR solution structures of Bi-stranded abasic site lesions in DNA. *Biochemistry* **2008**, *47*, 11909–11919.
[55] Chen, J.; Dupradeau, F. Y.; Case, D. A.; Turner, C. J.; Stubbe, J. DNA oligonucleotides with A, T, G or C opposite an abasic site: structure and dynamics. *Nucleic Acids Res.* **2008**, *36*, 253–262.
[56] Aramini, J. M.; Mujeeb, A.; Germann, M. W. NMR solution structures of [d(GCGAAT-3′-3′-alphaT-5′-5′-CGC)2] and its unmodified control. *Nucleic Acids Res.* **1998**, *26*, 5644–5654.
[57] Ide, H.; Tedzuka, K.; Shimzu, H.; Kimura, Y.; Purmal, A. A.; Wallace, S. S.; Kow, Y. W. Alpha-deoxyadenosine, a major anoxic radiolysis product of adenine in DNA, is a substrate for Escherichia coli endonuclease IV. *Biochemistry* **1994**, *33*, 7842–7847.
[58] Séquin, U. Nucleosides and Nucleotides. Part 5. The stereochemistry of oligonucleotides consisting of 2′-deoxy-α-D-riboses, a study with DREIDING stereomodels. *Experientia* **1973**, *29*, 1059–1062.
[59] Morvan, F.; Rayner, B.; Imbach, J. L.; Chang, D. K.; Lown, J. W. Alpha-DNA-III. Characterization by high field 1H-NMR, antiparallel self-recognition and conformation of the unnatural hexadeoxyribonucleotides alpha-[d(CpApTpGpCpG)] and alpha-[d(CpGpCpApTpG)]. Alpha-oligodeoxynucleotides as potential

cellular probes for gene control. *Nucleic Acids Res.* **1987**, *15*, 4241–4255.
[60] Morvan, F.; Rayner, B.; Imbach, J. L.; Lee, M.; Hartley, J. A.; Chang, D. K.; Lown, J. W. Alpha-DNA-V. Parallel annealing, handedness and conformation of the duplex of the unnatural alpha-hexadeoxyribonucleotide alpha-[d(CpApTpGpCpG)] with its beta-complement beta-[d(GpTpApCpGpC)] deduced from high field 1H-NMR. *Nucleic Acids Res.* **1987**, *15*, 7027–7044.
[61] Lancelot, G.; Guesnet, J. L.; Roig, V.; Thuong, N. T. 2D-NMR studies of the unnatural duplex alpha-d(TCTAAAC)-beta-d(AGATTTG). *Nucleic Acids Res.* **1987**, *15*, 7531–7547.
[62] Gmeiner, W. H.; Rayner, B.; Morvan, F.; Imbach, J. L.; Lown, J. W. Structure and conformation in solution of the parallel-stranded hybrid alpha-d(CGCAATTCGC).beta-d(GCGTTAAGCG) by high-resolution 2D NMR. *J. Biomol. NMR* **1992**, *2*, 275–288.
[63] Aramini, J. M.; Cleaver, S. H.; Pon, R. T.; Cunningham, R. P.; Germann, M. W. Solution structure of a DNA duplex containing an α-anomeric adenosine: insights into substrate recognition by Endonuclease IV. *J. Mol. Biol.* **2004**, *338*, 77–91.
[64] Johnson, C. N.; Spring, A. M.; Desai, S.; Cunningham, R. P.; Germann, M. W. DNA sequence context conceals alpha-anomeric lesions. *J. Mol. Biol.* **2012**, *416*, 425–437.
[65] Aramini, J. M.; Kalisch, B. W.; Pon, R. T.; van de Sande, J. H.; Germann, M. W. Structure of a DNA duplex that contains α-anomeric nucleotides and 3′ – 3′ and 5′ – 5′ phosphodiester linkages: coexistence of parallel and antiparallel DNA. *Biochemistry* **1996**, *35*, 9355–9365.
[66] Aramini, J. M.; van de Sande, J. H.; Germann, M. W. Spectroscopic and thermodynamic studies of DNA duplexes containing α-anomeric C, A, and G nucleotides and polarity reversals: coexistence of localized parallel and antiparallel DNA. *Biochemistry* **1997**, *36*, 9715–9725.
[67] Aramini, J. M.; Germann, M. W. Solution structure of a DNA · RNA hybrid containing an α-anomeric thymidine and polarity reversals: d(ATGG-3′-3′-αT-5′-5′-GCTC) · r(gagcaccau)†,‡. *Biochemistry* **1999**, *38*, 15448–15458.
[68] Aramini, J. M.; Mujeeb, A.; Ulyanov, N. B.; Germann, M. W. Conformational dynamics in mixed alpha/beta-oligonucleotides containing polarity reversals: a molecular dynamics study using time-averaged restraints. *J. Biomol. NMR* **2000**, *18*, 287–302.
[69] Nick McElhinny, S.; Kumar, D.; Clark, A.; Watt, D.; Watts, B.; Lundström, E.; Johansson, E.; Chabes, A.; Kunkel, T. Genome instability due to ribonucleotide incorporation into DNA. *Nat. Chem. Biol.* **2010**, *6*, 774–781.
[70] Hsiang-Chih Chiu, K. D. K., Marina Evich, Annie L. Lesiak, Markus W. Germann, Angelo Bongiorno, Elisa Reido, and Francesca Storici. RNA intrusions change DNA elastic properties and structure. *Nanoscale* **2014**, *6*, 10009–10017.
[71] Evich, M.; Spring-Connell, A. M.; Storici, F.; Germann, M. W. Structural Impact of Single Ribonucleotide Residues in DNA. *ChemBioChem* **2016**, *17*, 1968–1977.
[72] Case, D. A.; Babin, V.; Berryman, J. T.; Betz, R. M.; Cai, Q.; Cerutti, D. S.; Cheatham, T. E.; Darden, T. A.; Duke, R. E.; Gohlke, H.; et al. Amber 14; University of California: San Francisco, 2014.
[73] Zgarbová, M.; Luque, F. J.; Šponer, J.; Cheatham, T. E.; Otyepka, M.; Jurečka, P. Toward improved description of DNA backbone: revisiting epsilon and zeta torsion force field parameters. *J. Chem. Theory Comput.* **2013**, *9*, 2339–2354.
[74] Layzer, J. M.; McCaffrey, A. P.; Tanner, A. K.; Huang, Z.; Kay, M. A.; Sullenger, B. A. In vivo activity of nuclease-resistant siRNAs. *RNA* **2004**, *10*, 766–771.
[75] Sipa, K.; Sochacka, E.; Kazmierczak-Baranska, J.; Maszewska, M.; Janicka, M.; Nowak, G.; Nawrot, B. Effect of base modifications on structure, thermodynamic stability, and gene silencing activity of short interfering RNA. *RNA* **2007**, *13*, 1301–1316.
[76] Egli, M.; Pallan, P. S. Crystallographic studies of chemically modified nucleic acids: a backward glance. *Chem. Biodivers.* **2010**, *7*, 60–89.
[77] Lesnik, E. A.; Freier, S. M. What affects the effect of 2′-alkoxy modifications? 1. Stabilization effect of 2′-methoxy substitutions in uniformly modified DNA oligonucleotides. *Biochemistry* **1998**, *37*, 6991–6997.
[78] Wohlrab, F.; Haertlé, T.; Trichtinger, T.; Guschlbauer, W. 2′-Deoxy-2′-fluorouridine-5′-phosphate: an alternative substrate for thymidylate synthetase from Escherichia coli K12. *Nucleic Acids Res.* **1978**, *5*, 4753–4759.
[79] Barchi, J. J., Jr.; Jeong, L. S.; Siddiqui, M. A.; Marquez, V. E. Conformational analysis of the complete series of 2′ and 3′ monofluorinated dideoxyuridines. *J. Biochem. Biophys. Methods* **1997**, *34*, 11–29.
[80] Kawasaki, A. M.; Casper, M. D.; Freier, S. M.; Lesnik, E. A.; Zounes, M. C.; Cummins, L. L.; Gonzalez, C.; Cook, P. D. Uniformly modified 2′-deoxy-2′-fluoro phosphorothioate oligonucleotides as nuclease-resistant antisense compounds with high affinity and specificity for RNA targets. *Eur. J. Med. Chem.* **1993**, *36*, 831–841.
[81] Deleavey, G. F.; Watts, J. K.; Alain, T.; Robert, F.; Kalota, A.; Aishwarya, V.; Pelletier, J.; Gewirtz, A. M.; Sonenberg, N.; Damha, M. J. Synergistic effects between analogs of DNA and RNA improve the potency of siRNA-mediated gene silencing. *Nucleic Acids Res.* **2010**, *38*, 4547–4557.
[82] Yazbeck, D. R.; Min, K.-L.; Damha, M. J. Molecular requirements for degradation of a modified sense RNA strand by Escherichia coli ribonuclease H1. *Nucleic Acids Res.* **2002**, *30*, 3015–3025.
[83] Damha, M. J.; Wilds, C. J.; Noronha, A.; Brukner, I.; Borkow, G.; Arion, D.; Parniak, M. A. Hybrids of RNA and Arabinonucleic Acids (ANA and 2′F-ANA) are substrates of Ribonuclease H. *J. Am. Chem. Soc.* **1998**, *120*, 12976–12977.
[84] Kalota, A.; Karabon, L.; Swider, C. R.; Viazovkina, E.; Elzaghеid, M.; Damha, M. J.; Gewirtz, A. M. 2′-Deoxy-2′-fluoro-β-d-arabinonucleic acid (2′F-ANA) modified oligonucleotides (ON) effect highly efficient, and persistent, gene silencing. *Nucleic Acids Res.* **2006**, *34*, 451–461.
[85] Ikeda, H.; Fernandez, R.; Wilk, A.; Barchi, J. J.; Huang, X.; Marquez, V. E. The effect of two antipodal fluorine-induced sugar puckers on the conformation and stability of the Dickerson-Drew dodecamer duplex [d(CGCGAATTCGCG)]2. *Nucleic Acids Res.* **1998**, *26*, 2237–2244.
[86] Berger, I.; Tereshko, V.; Ikeda, H.; Marquez, V. E.; Egli, M. Crystal structures of B-DNA with incorporated 2′-deoxy-2′-fluoro-arabino-furanosyl thymines: implications of conformational preorganization for duplex stability. *Nucleic Acids Res.* **1998**, *26*, 2473–2480.
[87] Teplova, M.; Wilds, C. J.; Wawrzak, Z.; Tereshko, V.; Du, Q.; Carrasco, N.; Huang, Z.; Egli, M. Covalent incorporation of selenium into oligonucleotides for X-ray crystal structure determination via MAD: proof of principle. Multiwavelength anomalous dispersion. *Biochimie* **2002**, *84*, 849–858.
[88] Du, Q.; Carrasco, N.; Teplova, M.; Wilds, C. J.; Egli, M.; Huang, Z. Internal derivatization of oligonucleotides with selenium for X-ray crystallography using MAD. *J. Am. Chem. Soc.* **2002**, *124*, 24–25.

[89] Pallan, P. S.; Egli, M. Selenium modification of nucleic acids: preparation of oligonucleotides with incorporated 2′-SeMe-uridine for crystallographic phasing of nucleic acid structures. *Nat. Protoc.* **2007**, *2*, 647–651.
[90] Thompson, R. A.; Spring, A. M.; Sheng, J.; Huang, Z.; Germann, M. W. The importance of fitting in: conformational preference of Selenium 2′ modifications in nucleosides and helical structures. *J. Biomol. Struct. Dyn.* **2015**, *33*, 289–297.
[91] Kumar, R.; Singh, S. K.; Koshkin, A. A.; Rajwanshi, V. K.; Meldgaard, M.; Wengel, J. The first analogues of LNA (locked nucleic acids): phosphorothioate-LNA and 2′-thio-LNA. *Bioorg. Med. Chem. Lett.* **1998**, *8*, 2219–2222.
[92] Astakhova, I. K.; Wengel, J. Scaffolding along nucleic acid duplexes using 2′-amino-locked nucleic acids. *Acc. Chem. Res.* **2014**, *47*, 1768–1777.
[93] Sorensen, M. D.; Kvaerno, L.; Bryld, T.; Hakansson, A. E.; Verbeure, B.; Gaubert, G.; Herdewijn, P.; Wengel, J. Alpha-L-ribo-configured locked nucleic acid (alpha-L-LNA): synthesis and properties. *J. Am. Chem. Soc.* **2002**, *124*, 2164–2176.
[94] Kumar, N.; Nielsen, K. E.; Maiti, S.; Petersen, M. Triplex formation with alpha-L-LNA (alpha-L-ribo-configured locked nucleic acid). *J. Am. Chem. Soc.* **2006**, *128*, 14–15.
[95] Koshkin, A. A.; Nielsen, P.; Meldgaard, M.; Rajwanshi, V. K.; Singh, S. K.; Wengel, J. LNA (Locked Nucleic Acid): An RNA mimic forming exceedingly stable LNA:LNA duplexes. *J. Am. Chem. Soc.* **1998**, *120*, 13252–13253.
[96] Grunweller, A.; Hartmann, R. K. Locked nucleic acid oligonucleotides: the next generation of antisense agents? *BioDrugs* **2007**, *21*, 235–243.
[97] Di Giusto, D. A.; King, G. C. Strong positional preference in the interaction of LNA oligonucleotides with DNA polymerase and proofreading exonuclease activities: implications for genotyping assays. *Nucleic Acids Res.* **2004**, *32*, e32–e32.
[98] Wahlestedt, C.; Salmi, P.; Good, L.; Kela, J.; Johnsson, T.; Hökfelt, T.; Broberger, C.; Porreca, F.; Lai, J.; Ren, K.; et al. Potent and nontoxic antisense oligonucleotides containing locked nucleic acids. *Proc. Natl. Acad. Sci. U.S.A.* **2000**, *97*, 5633–5638.
[99] Aramini, J. M.; Germann, M. W. NMR studies of DNA duplexes containing alpha-anomeric nucleotides and polarity reversals. *Biochem. Cell Biol.* **1998**, *76*, 403–410.
[100] Rait, V. K.; Shaw, B. R. Boranophosphates support the RNase H cleavage of polyribonucleotides. *Antisense Nucleic Acid Drug Dev.* **1999**, *9*, 53–60.
[101] Stein, C. A.; Subasinghe, C.; Shinozuka, K.; Cohen, J. S. Physicochemical properties of phosphorothioate oligodeoxynucleotides. *Nucleic Acids Res.* **1988**, *16*, 3209–3221.
[102] Cummins, L.; Graff, D.; Beaton, G.; Marshall, W. S.; Caruthers, M. H. Biochemical and physicochemical properties of phosphorodithioate DNA. *Biochemistry* **1996**, *35*, 8734–8741.
[103] Wang, J. X.; Sergueev, D. S.; Shaw, B. R. The effect of a single boranophosphate substitution with defined configuration on the thermal stability and conformation of a DNA duplex. *Nucleosides Nucleotides Nucleic Acids* **2005**, *24*, 951–955.
[104] Johnson, C. N.; Spring, A. M.; Sergueev, D.; Shaw, B. R.; Germann, M. W. Structural basis of the RNase H1 activity on stereo regular borano phosphonate DNA/RNA hybrids. *Biochemistry* **2011**, *50*, 3903–3912.
[105] Mujeeb, A.; Reynolds, M. A.; James, T. L. High-resolution NMR of an antisense DNA x RNA hybrid containing alternating chirally pure Rp methylphosphonates in the DNA backbone. *Biochemistry* **1997**, *36*, 2371–2379.
[106] Reynolds, M. A.; Hogrefe, R. I.; Jaeger, J. A.; Schwartz, D. A.; Riley, T. A.; Marvin, W. B.; Daily, W. J.; Vaghefi, M. M.; Beck, T. A.; Knowles, S. K.; Klem, R. E.; Arnold, L. J., Jr. Synthesis and thermodynamics of oligonucleotides containing chirally pure R(P) methylphosphonate linkages. *Nucleic Acids Res.* **1996**, *24*, 4584–4591.
[107] Gonzalez, C.; Stec, W.; Reynolds, M. A.; James, T. L. Structure and dynamics of a DNA.RNA hybrid duplex with a chiral phosphorothioate moiety: NMR and molecular dynamics with conventional and time-averaged restraints. *Biochemistry* **1995**, *34*, 4969–4982.
[108] Hoppins, J. J.; Gruber, D. R.; Miears, H. L.; Kiryutin, A. S.; Kasymov, R. D.; Petrova, D. V.; Endutkin, A. V.; Popov, A. V.; Yurkovskaya, A. V.; Fedechkin, S. O.; Brockerman, J. A.; Zharkov, D. O.; Smirnov, S. L. 8-Oxoguanine affects DNA backbone conformation in the EcoRI recognition site and inhibits its cleavage by the enzyme. *PLoS One* **2016**, *11*, e0164424.
[109] Fadda, E.; Pomès, R. On the molecular basis of uracil recognition in DNA: comparative study of T-A versus U-A structure, dynamics and open base pair kinetics. *Nucleic Acids Res.* **2011**, *39*, 767–780.